Creative Method of Electron Exchange Magnitude (EEM) for Determination of Band Edges in PbS QDs

Heidaripour, Ashraf*[+]

Department of Chemistry, Payame Noor University, Tehran, I.R. IRAN

ABSTRACT: *Determining the band edges of Quantum Dots (QDs) in electrolytes with different redox is still a serious challenge for many researchers. A new and innovative method to trace Valence Band (VB) and Conduction Band (CB) edges is Electron Exchange Magnitude (EEM) determination with logarithmic scaling in Cyclic Voltammetry (CV) curves. The EEM method is an adaptation of the Tafel method, which determines the equilibrium currents in the logarithmic scale in the potential current curves. Accordingly, the equilibrium currents on the surface of QDs can be related to the currents occurring at the band edges. Since the band gap varies with the size of the QDs, the shift of the band edges occurs as the size of the QDs changes. In this study, PbS QDs were deposited on ITO/ZnO by the SILAR method and considered as a photoanod. The band edges were investigated by EEM method in electrolytes with and without Sulfide polysulfide redox. In this way, the minimum value of EEM in the anodic and cathodic range was considered as the VB and CB edges, respectively. Investigations show that some results of this research are in good agreement with the observations and results of others in matters such as determining the PbS QDs bandgap, although there are significant differences in determining the exact position of the band edges.*

KEYWORDS: *Electron Exchange Magnitude (EEM); PbS QDs; Band edges; Cyclic voltammetry; Logarithmic scale.*

INTRODUCTION

PbS QDs used for QD solar cells have received considerable attention owing to their huge bandgap tunable and multiple-exciton generation effect [1]. In general, in the QD solar cells, three components exist photoanode, cathode, and electrolyte-containing redox. The n-type QDs deposited on Wide Bandgap Semiconductor (WBS) like TiO_2, all on the conductive glass, are used as the photoanode. The cathode is often a p-type semiconductor deposited on the conductive glass or is a platinized electrode. Finally, a suitable redox system in electrolyte completes an electrolytic connection between photoanode and cathode [2-6]. In this way, the QDs have two electronic connections on both sides, with the redox system in electrolyte and the other with a WBS as a substrate [6]. According to Grischer's model, the electron exchange between the redox and QDs occurs at the band edges so Electron Exchange Magnitude (EEM) is related to the band edges position in QDs and redox potential [7]. In the ideal conditions, electrons would transfer from the redox system to the VB edge of the QDs, and then electrons in VB are photo-excited to the CB edge of the QDs and then transfer to the CB edge of a WBS where

***** *To whom correspondence should be addressed.*
+ E-mail: ashrafheidaripour@gmail.com
1021-9986/2023/6/1832-1841 10/$/6.00

accede to towards the cathode via circuit. Therefore, it is appropriate that in the designation of the QD solar cells the redox systems with potential close to the VB of the QDs are chosen. In addition, it is ideal that the CB edge of the WBS to be near the CB edge of QDs [2]. So it is desirable to change and determine the exact position of VB and CB edge of the QDs and WBS to provide the best condition for electron transfer. Determining the band edges is still one of the serious challenges that for which many practical and formulaic solutions have been proposed [8].

According to reports the VB and CB edges of the PbS QDs is approximately at +0.4 and -1.0V versus standard calomel electrode (SCE), and at -4.0 and -5.4 versus electron volt (eV), Fig.1. But the band edges can change when size, shape and density change. Also, the VB, CB and bandgap energy of WBSs have been detected by researchers [9]. As can be seen in Fig. 1 the CB edge of some of WBSs is in a suitable position, i.e. more positive than CB edge of PbS QDs. Then electrons could easily transfer from PbS QDs to the WBS via CB edge when its surface is exposed to light. The ZnO is an appropriate WBS due to its high absorption coefficient and appropriate CB edge position [10-13].

On the other hand, the PbS QDs would be in contact with the electrolyte containing a suitable redox. Since the PbS QDs is unstable in acidic electrolyte so alkaline electrolyte is almost always used for PbS QDs [14]. In alkaline electrolyte, hydroxide ($[OH^-]$=1M) oxides into O_2 at +0.64V/SCE (Fig.1). Although this redox (OH^-/O_2) is potentially close to the VB of the PbS QDs, but is not suitable redox because of irreversibility [2, 5, 6, 15].

Sulfide polysulfide (S^{2-}/S_n^{2-}) redox system is an important redox in QD-solar cells. The potential of S^{2-}/S_n^{2-} redox in aqueous system is at -0.84V/SCE (Fig.1) [14]. This potential is near the CB edge of the PbS QDs while in the best conditions the redox potential would be near the VB edge. But we used S^{2-}/S_n^{2-} redox in this study due to lack of access to proper redox [16]. Therefore, in first step determining the accurate position of the CB and VB in semiconductors and exact potential of different redox can be helpful. The band edges of the semiconductor and its band gap can be determined in various ways, that one of them is Cyclic Voltammetry (CV) method [17, 18]. In CV method which is sweep of current (J) versus potential (V), the band edges can be roughly estimated from the first

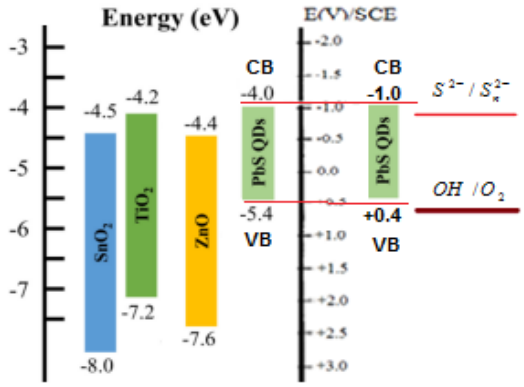

Fig. 1: VB and CB edges of the some of WBSs and PbS QDs [9].

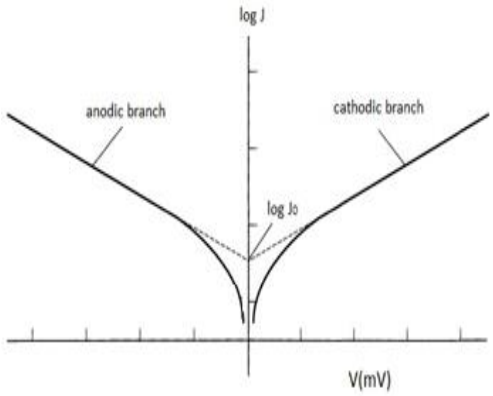

Fig. 2: Tafel plot for anodic and cathodic branches of the current-over potential curve [19].

anodic and cathodic peaks [17]. But in our proposed method, the band edges can be tracked and find with higher accuracy. In this new method the logarithmic scale of CV, i.e. (log J)/V is used to determine Electron Exchange Magnitude (EEM) and track the VB and CB edges through the least EEM. The proposed method of determination of the least EEM from logarithmic scale of CV for tracking the band edges is completely new and its basic idea is adapted from the Tafel method in corrosion field. In Tafel method the log J versus V is plotted (Fig. 2) and an anodic and a cathodic linear branch with different slope is obtained in which both linear segments extrapolate to an intercept of the log J_0 [19].

The J_0 is the least equilibrium current. Accordingly, in the logarithmic scale of CV curves the intercepts show equilibrium currents in electrode surface at anodic and cathodic ranges. According to Grischer's model, equilibrium current, J_0, at the surface of semiconductor

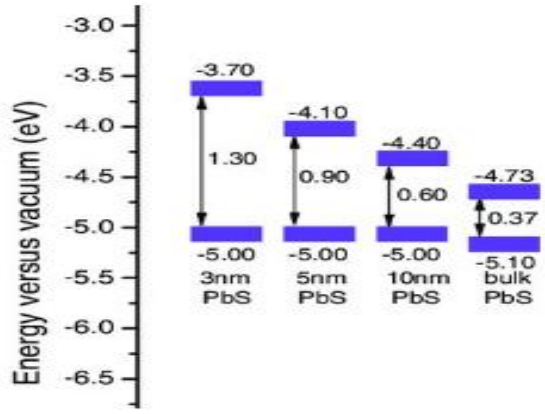

Fig. 3: Relationships between particle size and bandgap energy [21].

occurs only in condition of minimal band bending [7]. As a reminder, in semiconductors Fermi level of electrons is closer to the CB while the quasi-Fermi level of holes is closer to the VB. So the equilibrium current via CB ($\log J_0^c$) occurs in negative potential and equilibrium current via VB ($\log J_0^a$) occurs in positive potential. Therefore, the potential in which $\log J_0^c$ and $\log J_0^a$ is located are CB and VB edges, respectively. Difference between CB and VB edges is a criterion of band gap energy [20].

In Fig. 3 the relationship between the bandgap energy of PbS QDs and particle size is illustrated in vacuum scale (eV). When particle size decreases from bulk to 3nm, bandgap energy increases from 0.37 to 1.3eV, respectively. According to this research Bandgap increases only by moving the CB to more energetic regions, and the VB remains almost constant [21].

The value of bandgap energy can be compared with that obtained from the UV-visible spectroscopy technique. UV-visible spectroscopy is used to identify the wavelength of the first exciton in PbS QDs and measure bandgap energy. When the size of QDs decreases, the absorption edge moves toward shorter wavelengths and energy gap increases [22]. Although this comparison is not very accurate because in the spectroscopic method the electrode is outside the electrolyte and in our proposed method the electrode is inside the alkaline electrolyte with assumption that electrode surface is chemically stable [23].

In this new proposed method (EEM), the value of log J is considered as a measure of electron exchange and its magnitude can be related to the distance between applied potential and band edges. In equilibrium condition the electron exchange occurs through the band edges with the least energy so current J is minimal ($J= J_0$) and in no equilibrium condition the electron exchange increases exact similar to Tafel plots.

EXPRIMENTAL SECTION

Materials and instruments

Indium tin oxide (ITO) with resistivity of 22Ω was purchased from Dyesol and cut to surface of $2cm^2$. Materials of $Pb(NO_3)_2$, $Zn(NO_3)_2$, Na_2S, S, and NaOH all were analytical grade (Merck) and were used without further purification. All electrochemical measurements were carried out in a conventional three electrode cell powered by a potentiostat/ galvanostat (EG&G, model 273 A) that was run by a PC through M 270 and M398 software via a GPIB interface, and a frequency response analyzer (EG&G, model 1025). Images of scanning electron microscope (SEM) were obtained with VEGA\ TESCAN. Zinc oxide (ZnO) was electrodeposited on the ITO during two different time via chronoamperometry (CA) technique in 0.1M $Zn(NO_3)_2$ solution at -0.85V/SCE. At -0.85V/SCE on the ITO surface nitrate ions (NO_3^-) reduce to OH^- and immediately OH^- ions along with Zn^{2+} ions, form ZnO deposition on the ITO (ITO/ZnO) [10, 24]. For investigation of ZnO band edges in an alkaline electrolyte, two samples of ITO/ZnO were prepared during 800s and 1200s at 25°C (800s-sample and 1200s-sample).

Preparation of electrodes

For preparation of ITO/ZnO/PbS electrodes, PbS QDs was deposited on the ITO/ZnO (1200s-sample). Deposition was performed using successive ionic layer adsorption and reaction (SILAR) method which is one of the best method for PbS QDs preparation [22, 25]. In any SILAR stage, the ITO/ZnO was immersed for 1 minute into solution of 0.1M $Pb(NO_3)_2$, distilled water and solution of 0.1M Na_2S respectively. In any SILAR stage one PbS layer (PbS-1layer) forms. To obtain the higher thickness the SILAR stages were repeated two (PbS-2layer), three (PbS-3layer) and four (PbS-4layer) times.

RESULT AND DISCUSSION

Surface Properties of ITO/ZnO/PbS

The SEM image of surface of blank electrode surface (ITO) is shown in Fig. 4a and surface of ITO/ZnO/PbS-

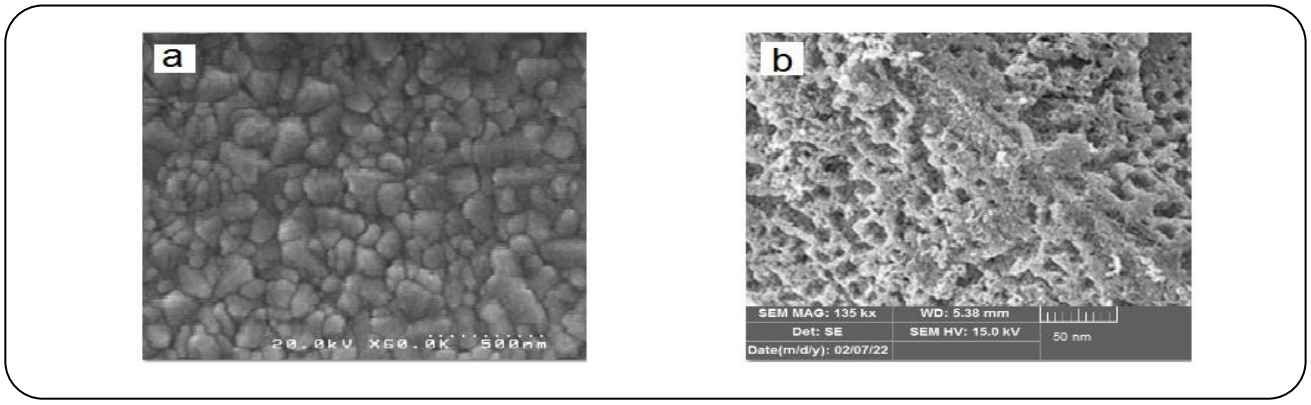

Fig. 4: SEM of electrode surface of a) ITO, b) ITO/ZnO/PbS-4layer.

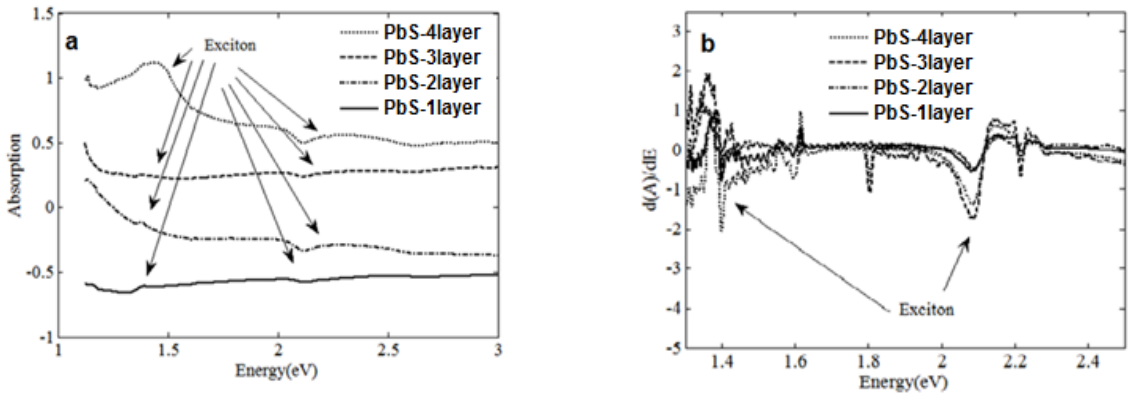

Fig. 5: a) UV-visible spectrum of ITO/ZnO/PbS-1 to 4layer, b) derivation of spectrum.

4layer is shown in Fig. 4b. As can be seen, a thin layer of ZnO has been formed with nanometric porosity that PbS QDs can be settled down inside.

Spectroscopic Properties of ITO/ZnO/PbS

UV-visible spectroscopy has been used to investigate the optical properties and band gap energy of PbS QDs. Fig. 5a shows that absorption increases with increasing PbS QDs thickness but the first absorption edge for all samples is located at 1.4eV which is related to formation of the first exciton and equivalent to bandgap energy. With reference to Fig. 3a, and based on reports [21, 26], the band gap energy of 1.4eV is related to formation of electron-hole in PbS QDs with size of 2.5-3 nm. To better identify the band gap energy, the first derivative of the UV-Visible absorption spectrum is shown in Fig. 5b. It seems that the UV-visible spectroscopy method is not a good method for this case Because it does not show a noticeable difference in band gap energy with the change of PbS QDs thickness. On the other hand the UV-visible spectroscopy is performed in the air environment outside the electrolyte, which may cause the edges of the VB and CB to be different from that in the electrolyte.

Electrochemical properties of ITO/ZnO/PbS

The open circuit potential (OCP) of the ITO/ZnO/PbS-1 to 4layer in alkaline electrolyte (0.5M NaOH) is about -0.7V/SCE. The OCP is a criterion of the Fermi level of semiconductor in electrolyte [2] so Fermi level of PbS is almost similar in PbS-1 to 4layer. The OCP of the ITO/ZnO/PbS-1 to 4layer in alkaline electrolyte containg S^{2-}/S_n^{2-} is -0.70V/SCE which is similar to that in alkaline electrolyte without redox. This shows that S^{2-}/S_n^{2-} redox has not decreased PbS QDs Fermi level. The postulated potential for S^{2-}/S_n^{2-} redox is -0.84V/SCE (Fig. 1) [14].

Investigation of EEM method on ITO/ZnO

To find the band edges of ZnO by EEM method the CV curves of ITO/ZnO were performed in solution of

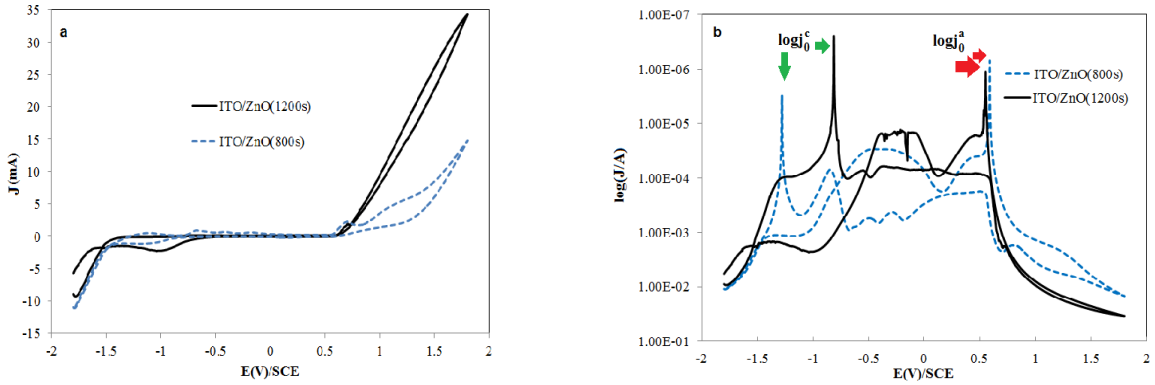

Fig.6: (a) CV curves of the 800s and 1200s-sample in alkaline electrolyte, (b) Logarithmic scale of CVs.

5.0 M NaOH, Fig. 6a. The CV curves significantly show differences at two ends of the CVs. An increase of anodic and cathodic current in 1200s-sample with respect to 800s-sample is related to the more surface of ZnO. To find the ZnO band edges from the CV curves, the logarithm of the CVs, (log J)/V, has been derived and shown in Fig.6b in which the minimums of EEM have been illustrated with red arrow in anodic range and with green arrow in cathodic range. As is seen, log J_0^a is observed at +0.60V/SCE in both samples, while log J_0^c is observed at -1.3 and -0.7V/SCE for 800s-sample and 1200s-sample, respectively. It shows that the CB edge is shifted towards positive potential as the time of the electrodeposition changes from 800s to 1200s.This displacement is ideal because when the CB edge of ZnO is enough positive, electrons could easily transfer from PbS QDs to CB of ZnO [27].

Investigation of EEM method on ITO/ZnO/PbS in electrolyte without redox

Fig.7a shows the CV curves of the ITO/ZnO/PbS-1 to 4layer in alkaline electrolyte with SCE as a reference electrode and against the carbon C as a counter electrode. A clear difference is seen at the CVs' ends, so that, an increase of SILAR stages leads to an increase of the current intensity. At logarithmic scale, (log J)/V, only the anodic scan is shown to avoid the crowding of the graph, Fig. 7b. The minimums of EEM have been illustrated with red arrow in anodic range and with green arrow in cathodic range. It is obvious that by increasing the layers of PbS the potential of log J_0^a changes from +0.44 to 0.00V/SCE, while log J_0^c is fixed at around -0.9V/SCE, Fig.7b. These observations show that the CB edge of PbS QDs is fixed at -0.9V/SCE, contrary to some reports that the VB is fixed at PbS QDs [21]. Difference between CB and VB for PbS-4layer is 0.90V which is a creterion of band gap energy. The value of log J_0^c (=0.001) is very higher than log J_0^a (=0.000001) which is thought-provoking and debatable.

As before mentioned the OCP of the ITO/ZnO/PbS-1 to 4layer is -0.70V/SCE, so the PbS Fermi level is at -0.70V/SCE near PbS CB edge which confirms the n-type PbS has been formed [28, 29]. According to Fig.7b, it is clear that by changing PbS thickness the VB edge displaces. Displacement of the VB edge as much as desired provides the possibility of using other redox system too [30, 31].

Referal to Fig.6b and Fig.6b, the CB edge of ZnO (1200s sample) is at -0.70V/SCE and that for PbS QDs is at -0.90V/SCE. The lower CB edge of ZnO than that of PbS QDs is ideal because electrons could easily transfer from PbS QDs to ZnO with minimal energy.

Investigation of photocurrent in ITO/ZnO/PbS in electrolyte without redox

The J-V curves of the ITO/ZnO/PbS-1 to 4layer have been plotted from OCP= -0.70V to 0.00V with respect to the SCE and against the carbon C in 0.5M NaOH solution in dark and under light, Fig. 8a and Fig.8b. In dark during the potential range the current is totally anodic. At -0.70V/SCE current intensity for all samples (PbS-1 to 4layer) is minimum and equals to -0.18mA. Also, the current intensity at 0.0V/SCE is from 4.63 to 7.93mA for PbS-1 to 4layer, respectively, Fig.8a. The maximum

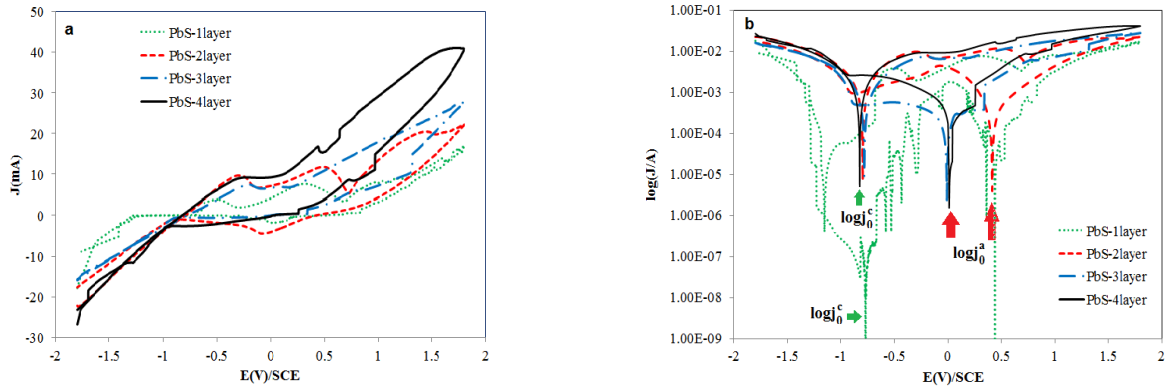

Fig. 7: (a) CV curves of the ITO/ZnO/PbS-1 to 4layer in alkaline electrolyte, (b) Logarithmic scale of CVs.

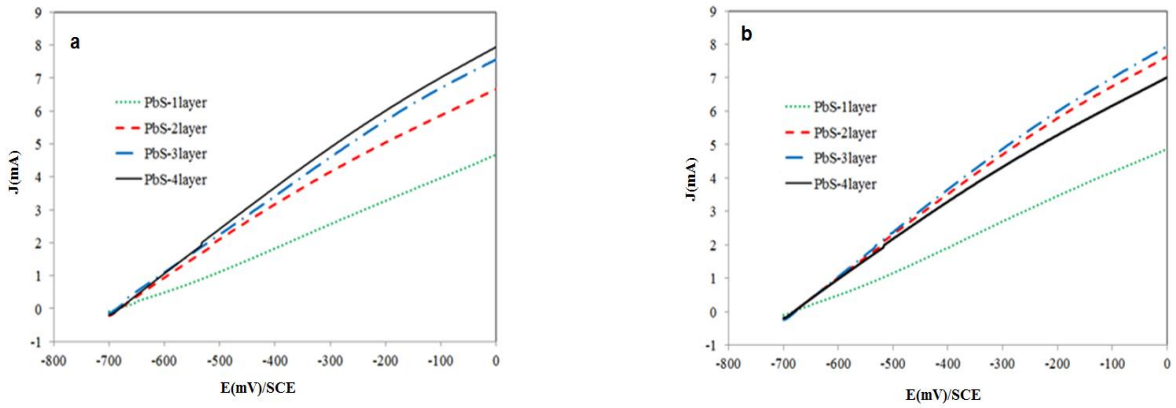

Fig. 8: J-V curves of the ITO/ZnO/PbS-1to 4layer) alkaline electrolyte a) in dark, b) under light s.

photocurrent is 200µA for PbS-1 to 3layer. For PbS-4layer under light a decrease in current is seen which is may be related to destruction of the PbS QDs surface, Fig. 8b.

Investigation of EEM method on ITO/ZnO/PbS in electrolyte containing redox

According to Fig.9a the CVs of the ITO/ZnO/PbS-1 to 4layer have been plotted versus SCE as a reference electrode and against the carbon C as a counter electrode in 0.5M NaOH solution containg S^{2-}/S_n^{2-}. The aim of this experiment is to achieve more data about CB and VB edges in PbS QDs. A clear difference is seen in the two ends of CVs, so that by increasing the number of PbS layers the current flow rate increases. The (log J)/V curves has been shown in Fig. 9b. The minimums of EEM have been illustrated with red arrow in anodic range and with green arrow in cathodic range. The position of log J_0^c for ITO/ZnO/PbS-1 to 4layer is at -0.81V/SCE which demonestrated within an yellow ellipse. It shows that the CB edge of PbS QDs for all samples is fixed at about -0.81V/SCE in 0.5M NaOH solution containg S^{2-}/S_n^{2-}. This potential is 0.09V more positive than when there was no redox (Fig. 7b). Also, the potential displacement in log J_0^a is considerable and changes from -0.22 to +0.20V/SCE by increasing PbS layers (i.e. 0.40V displacement). Difference between CB and VB for PbS-4layer is 1.01V which is a creterion of band gap energy.

Investigation of photocurrent in ITO/ZnO/PbS in electrolyte containing redox

The J-V curves of the ITO/ZnO/PbS-1 to 4layer have been plotted in 0.5M NaOH solution containing S^{2-}/S_n^{2-} from OCP = -0.70V/SCE to 0.00V/SCE and against the carbon C in dark and under light, Fig. 10a and Fig. 10b. During these potential ranges the current is firstly cathodic until -300mV/SCE, then it converts to anodic mode in dark and under light. For the ITO/ZnO/PbS-

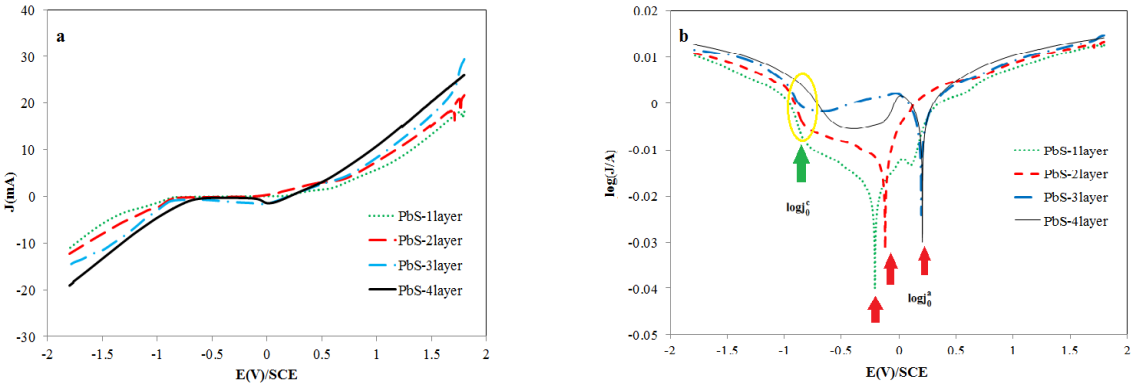

Fig. 9: CV curves of the electrode ITO/ZnO/PbS-1 to 4layer in alkaline electrolyte containg S^{2-}/S_n^{2-}, (b) Logarithmic scale of CVs.

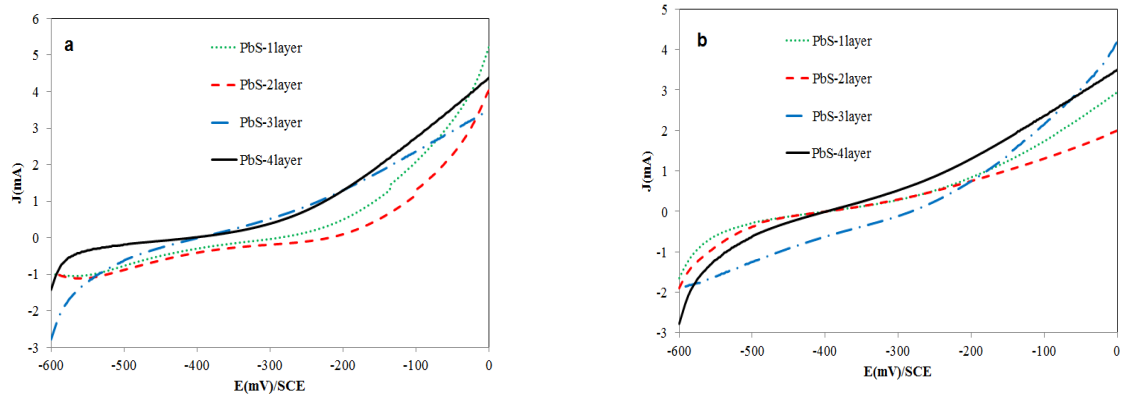

Fig. 10: I-V curves of electrode ITO/ZnO/PbS-1 to 4layer in electrolyte containg S^{2-}/S_n^{2-}, a) in dark, b) under light.

4layer and in dark, at -0.7V/SCE (OCP) and 0.00V/SCE the current is -3 and +3.5mA, respectively, Fig. 10a. In respect to Fig. 8a in which the current intensity at -0.7V/SCE (OCP) and 0.00V/SCE is -0.18 and 7.93mA, respectively, the presence of redox has reduced the current intensity at 0.00V/SCE but increased the current intensity at OCP. This phenomenon is due to the proximity of the S^{2-}/S_n^{2-} redox potential to the CB edge of PbS QDs.

These results can be interpreted more accurately by referring to Fig. 1. The proximity of the redox potential surface to the edge of the CB in PbS QDs results in better and more intense electron exchange at the OCP potential. These results lead us to the general conclusion that using the S^{2-}/S_n^{2-} redox for PbS QDs is not a good option because instead of exchanging electrons in the VB, which is desirable for QD solar cells, it exchanges electrons in the CB egde. In consequence no effective photo-current occurs. As can be seen in Fig. 10b, under light, no specific photo-current is observed, while in alkaline electrolyte without redox (Fig. 8b), the photo-current were much more pronounced because in which the potential of OH^-/O_2 (+0.64V/SCE) is near the VB edge of PbS QDs.

General results of redox effect on the ITO/ZnO/PbS

For better comparison, the results of Fig. 7b and 9b are summerized in table 1 and table 2, in which the VB, CB edges and band gaps of ITO/ZnO/PbS-1 to 4layer in alkaline electrolyte with and without S^{2-}/S_n^{2-} redox have been listed. As can be seen an obvious shift in the VB is observed in both conditions but the CB is almost constant. An increase in the number of PbS layers causes a decrease in the bandgap from 1.21 to 0.90eV in electrolyte without redox, table1. But in the presence of redox, this process becomes irregular, which can be attributed to the change of band edges, Table 2.

Table 1: VB, CB edge and band gap in alkaline electrolyte without redox.

	PbS-1layer	PbS-2layer	PbS-3layer	PbS-4layer
VB (V/SCE)	+0.44	+0.41	+0.01	+0.00
CB (V/SCE)	-0.77	-0.90	-0.9	-0.9
Band gap(eV)	1.21	1.31	0.91	0.90

Table 2: VB, CB edge and band gap in alkaline electrolyte containing redox.

	PbS-1layer	PbS-2layer	PbS-3layer	PbS-4layer
VB (V/SCE)	-0.22	-0.12	+0.20	+0.20
CB (V/SCE)	-0.81	-0.81	-0.81	-0.81
Band gap(eV)	1.03	0.93	1.01	1.01

CONCLUSIONS

Accurate determination of band edges using simple electrochemical methods can help in accurate and effective selection of suitable redox for PbS QD solar cells. For this purpose, the CV curves are a good method to find the edges of VB and CB. But due to Ambiguity in corresponding peaks, detection of the band edges is often associated with errors. In this article, by using the logarithmic scale of the CV curves, a new and innovative method is proposed for determining the band edges. The potential that Electron Exchange Magnitude (EEM) is at least is a good approximation for band edges position. These potentials as a measure of the equilibrium point where the electrons exchange by least energy between the band edges and redox have the same results as those reported in the articles. In this way, by using the EEM model similar to Tafel model the least EEM can easily be determined. These minima are closely related to the band edges, because when the applied potential to the electrode is exactly the same as the VB and CB edges, the band bending in semiconductor is minimal and the electron exchange takes place in equilibrium at low intensity.

Acknowledgments

In this research, I would like to thank the officials of the electrochemistry laboratory of KNT University of Technology for their laboratory services, and I would like to thank Professor Majid Jafarian for his sincere support.

Received : Jul. 22, 2022 ; Accepted : Oct. 24, 2022

REFERENCES

[1] Lu K., Wang Y., Liu Z., Han L., Shi G., Fang H., Chen J., Ye X., Chen S., Yang F., Shulga A. G., Wu T., Gu M., High-Efficiency PbS Quantum-Dot Solar Cells with Greatly Simplified Fabrication Processing *via* Solvent-Curing, *Adv. Mat*er., **30(25)**: 1707572 (2018).

[2] Bera D., Qian L., Tseng T.K., Holloway P.H. Quantum Dots and Their Multimodal Applications: A Review. *Mater.*, **3(4)**: 2260-2345 (2010).

[3] Debnath R., Tang J., Barkhouse D.A., Wang X., Andras G., Pattantyus-Abraham A.G., Brzozowski L., Levina L., Edward H. Sargent E.H., Ambient-Processed Colloidal Quantum Dot Solar Cells Via Individual Pre-Encapsulation of Nanoparticles, *J. Am. Chem. Soc.*, **132(17)**: 5952-5953 (2010).

[4] Jiao Y., Gao X., Lu J., Chen Y., Zhou J., Li X., A Novel Method for PbS Quantum Dot Synthesis, *Mater. Lett.*, **72**: 116-118 (2012).

[5] Jun H.K., Careem M.A., Arof A.K., A Suitable Polysulfide Electrolyte for CdSe Quantum Dot-Sensitized Solar Cells, *Int. J. Photoenergy*, **2013** (2013).

[6] Kamat P.V., Quantum Dot Solar Cells. Semiconductor Nanocrystals As Light Harvesters, *J. Phys. Chem. C*, **112(48)**: 18737-18753 (2008).

[7] Heidaripour A., Ajami N., Miandari S., Research of Gerischer Model in Transferring Electrons Between Energy States of CdS Thin Film and Ferro-Ferric Redox System, *Phys. Sci. Res. Int*, **3**:59-64 (2015).

[8] Shao Q., Lin H., Shao M., Determining Locations of Conduction Bands and Valence Bands of Semiconductor Nanoparticles Based on Their Band Gaps. *ACS Omega*, **5(18)**: 10297-10300 (2020).

[9] Zheng F., Liu Y., Ren W., Sunli Z., Xie X., Cui Y., Hao Y., Application of Quantum Dots in Perovskite Solar Cells, *Nanotechnology*, **32(48)**: 482003 (2021).

[10] Ajami N., Ehsani A., Babaei F., Heidaripour A., Electrosynthesis and Optical Modeling of ZnO nanostructures, *Iran. Chem. Commun.*, **3**: 85-92 (2015).

[11] Keis K., Magnusson E., Lindström H., Lindquist S.E., Hagfeldt A., A 5% Efficient Photoelectrochemical Solar Cell Based on Nanostructured ZnO Electrodes, *Sol. Energy Mater. Sol. Cells*, **73(1)**: 51-58 (2007).

[12] Martinson A.B.F., Elam J.W., Hupp J.T., Pellin M.J., ZnO Nanotube Based Dye-Sensitized Solar Cells, *Nano Lett.*, **7(8)**: 2183-2187 (2007).

[13] Tena-Zaera R., Elias J., Lévy-Clément C., ZnO Nanowire Arrays: Optical Scattering and Sensitization to Solar Light, *Appl. Phys. Lett.*, **93(23)**: 233119 (2008).

[14] Jovanovski V., González-Pedro V., Giménez S., Azaceta E., Cabañero G., Grande H., Tena-Zaera R., Mora-Seró I., Bisquert J., A Sulfide/Polysulfide-Based Ionic Liquid Electrolyte for Quantum Dot-Sensitized Solar Cells, *J. Am. Chem. Soc.*, **133(50)**: 20156-20159 (2011).

[15] Cuharuc A.S., Kulyuk L.L., Lascova R.I., Mitioglu A.A., Dikusar A.I., Electrochemical Characterization of Pbs Quantum Dots Capped with Oleic Acid and Pbs Thin Films-A Comparative Study, *Surface Engineering and Applied Electrochemistry*, **48(3)**: 193-211 (2012).

[16] Azevedo J., Seipp T., Burfeind J., Sousa C., Bentien A., Araújo J.P., Mendes A., Unbiased Solar Energy Storage: Photoelectrochemical Redox Flow Battery, *Nano Energy*, **22**: 396-405 (2016).

[17] Miandari S., Jafarian M., Mahjani M.G., Gobal F., Heidaripour A., Electrochemical Determination of CdS Band Edges and Semiconducting Parameters, *Bull. Chem. Soc. Jpn.*, **88(6)**: 814-820 (2015).

[18] Aderne R.E., Borges B.G.A.L., Ávila H.C., Kieseritzky F.V., Hellberg J., Koehler M., Cremona M., Roman L.S., Araujo C.M, Rocco M.L.M., Marchiori C.F.N., On the Energy Gap Determination of Organic Optoelectronic Materials: The Case of Porphyrin Derivatives, *Mater. Adv.*, **3(3)**: 1791-1803 (2022).

[19] Bard A.J., Faulkner L.R., "Electrochemical Methods: Fundamentals and Applications", Vol. 2. John Wiley & Sons Inc., New York (1980).

[20] Memming R., "Semiconductor Electrochemistry", John Wiley & Sons Inc. (2015).

[21] Du K., Liu G., Chen X.,Wang K., PbS Quantum Dots Sensitized TiO_2 Nanotubes for Photocurrent Enhancement. *J. Electrochem. Soc.*, **162(10)**: E251 (2015).

[22] Khurshid S., Latif H., Rasheed S., Sharif R., Sattar A., Amjad R.J., Enhancement in Absorption Spectrum by ITO Coated, Down Converting Glass as a Photoanode Substrate for Efficient PbS/CdS Quantum Dots Sensitized ZnO Nano-Rods Array Solar Cell, *Optical Materials*, **124**: 111991 (2022).

[23] Heidaripour A., Jafarian M., Gobal F., Mahjani M. G., Miandari S., Investigation of Pb/PbS a Positive Schottky Junction Formed oOn Conductive Glass in Contact with Alkaline Solution, *J. Appl. Phys.*, **116(3)**: 034906 (2014).

[24] Hajnorouzi A., Afzalzadeh R., Ghanati F., Ultrasonic irradiation effects on Electrochemical Synthesis of ZnO Nanostructures, *Ultrason. Sonochem.*, **21(4)**: 1435-1440 (2014).

[25] Murugesan R., Marimuthu K., Kasinathan K., An Investigation of SILAR Grown CdO Thin Films, *Iran. J. Chem. Chem. Eng. (IJCCE)*, **38(4)**: 11-17 (2019).

[26] Ding C., Zhang Y., Liu F., Nakazawa N., Huang Q., Hayase S., Ogomi Y., Toyoda T., Wang R., Shen Q., Recombination Suppression in PbS Quantum Dot Heterojunction Solar Cells by Energy-Level Alignment in the Quantum Dot Active Layers, *ACS Appl. Mater. Interfaces*, **10(31)**: 26142-26152 (2017).

[27] Janotti A., Van de Walle C.G., Native Point Defects in ZnO. *Phys. Rev. B*, **76**(16): 165202 (2007).

[28] Memming R., "Semiconductor Electrochemistry". John Wiley & Sons Inc. (2008).

[29] Bisquert J., Fabregat-Santiago F., Mora-Seró I., Garcia-Belmonte G., Barea E.M., Palomares E., A Review of Recent Results on Electrochemical Determination of the Density of Electronic States of Nanostructured Metal-Oxide Semiconductors and Organic Hole Conductors, *Inorg. Chim. Acta*, **361(3)**: 684-698 (2008).

[30] Bard A.J., Bocarsly A.B., Fan F.R.F., Walton E.G., Wrighton M.S., The Concept of Fermi Level Pinning at Semiconductor/Liquid Junctions. Consequences for Energy Conversion Efficiency and Selection of Useful Solution Redox Couples in Solar Devices, *J. Am. Chem. Soc*., **102(11)**: 3671-3677 (1980).

[31] Khan S.U.M, Kainthla R.C., Bockris J.O.M, The Redox Potential and the Fermi Level in Solution, *J. Phys. Chem.*, **91(23)**: 5974-5977 (1987).